

## Magnetic Properties of $\text{Fe}_x\text{V}_{3-x}\text{S}_4$ ( $0 \leq x \leq 2$ )

HIROSHI NOZAKI AND HIROAKI WADA

*National Institute for Research in Inorganic Materials, 1-1 Namiki,  
Sakura-mura, Niihari-gun, Ibaraki, 305, Japan*

Received September 16, 1982; in revised form November 8, 1982

The magnetic susceptibility data of  $\text{Fe}_x\text{V}_{3-x}\text{S}_4$  ( $0 \leq x \leq 2$ ) are reported in the temperature range between 4.2 and 1300 K. The behavior of the susceptibility at high temperatures changes significantly at the composition boundary  $x = 1.0$ . The magnitude of the effective magnetic moment remains unchanged at  $3.2 \mu_B$  in the composition range  $x < 1.0$ . It decreases with increasing iron content in the range  $> 1.0$ , and rapidly decreases for  $x$  close to 2.0. The  $c$  lattice parameter varies in a manner analogous to the change in magnetic moment. These phenomena suggest that metallic bonding forms between metal layers and that it becomes stronger with increasing  $x$ . The susceptibility measurements at low temperatures show that  $\text{Fe}_x\text{V}_{3-x}\text{S}_4$  is basically antiferromagnetic, although some of the  $\text{Fe}_x\text{V}_{3-x}\text{S}_4$  compounds become weakly ferromagnetic after cooling in a magnetic field. The origin of the weak ferromagnetism is briefly discussed.

### Introduction

Vanadium sulfides  $\text{VS}-\text{VS}_2$  with metal-deficient NiAs-like structures exhibit a wide variety of magnetic properties.  $\text{V}_3\text{S}_4$  which is one of the representative compounds in the V-S system is a weak itinerant antiferromagnet with a Néel temperature of about 8 K (1) and has no localized magnetic moment. On the other hand, the iron sulfide  $\text{Fe}_{1-x}\text{S}$  with the metal-deficient NiAs-like structure, which has a more limited range of nonstoichiometry than the V-S system, has a high Néel temperature and large localized magnetic moment, corresponding to the high-spin states of iron (2). Iron atoms substituted for vanadium in  $\text{VS}-\text{VS}_2$  have been thought to exist in a variety of states: high-spin or low-spin states, or states intermediate between localized and itinerant  $d$  electrons (3-5). In the ternary solid solution,  $\text{Fe}_x\text{V}_{3-x}\text{S}_4$ , the magnetic

properties of  $\text{FeV}_2\text{S}_4$  have been studied by magnetic susceptibility (6, 7) and Mössbauer effect experiments (3).  $\text{FeV}_2\text{S}_4$  is an antiferromagnet with a Néel temperature of 140 K; the susceptibility is very anisotropic (6). The iron was reported as being  $\text{Fe}^{2+}$  in the high-spin state. It was also reported that  $\text{Fe}_x\text{V}_{3-x}\text{S}_4$  between  $x = 0$  and  $x = 1.0$  is antiferromagnetic and that the Néel temperatures increase with increasing iron content (3). However, no composition dependence of magnetic parameters except for the Néel temperature is reported for  $\text{Fe}_x\text{V}_{3-x}\text{S}_4$ . It is necessary to examine the  $d$  states of iron in  $\text{Fe}_x\text{V}_{3-x}\text{S}_4$  over the whole range of composition through a magnetic investigation.

Recently, the phase relations of the ternary Fe-V-S system have been studied extensively (8-11) confirming that  $\text{Fe}_x\text{V}_{3-x}\text{S}_4$  has a structure isomorphous to  $\text{V}_3\text{S}_4$  in the whole range of composition between  $x = 0$

( $V_3S_4$ ) and  $x = 2.0$  ( $Fe_2VS_4$ ).  $V_3S_4$  (12) assumes a metal-deficient NiAs structure in which metal vacancies are involved in every second layer of metal atoms. These vacancies are in an ordered state at least at room temperature, resulting in a monoclinic structure. There exist two different metal sites in this structure, one of which, called the  $M_1$  site, lies in the metal-deficient layers (half-filled layers) and the other, called the  $M_2$  site, in the metallic layers. The arrangement of metal sites in the  $V_3S_4$  structure is shown in Fig. 1, where the intervening sulfur layers are omitted for clarity. The site distribution of Fe and V atoms in  $Fe_xV_{3-x}S_4$  was studied by the Mössbauer effect (13) as well as by neutron diffraction (14). Iron atoms substitute for the  $M_1$  sites successively with increasing iron content up to  $x = 1.0$  ( $FeV_2S_4$ ); at that point iron atoms fill the  $M_1$  sites completely. On further increasing  $x$ , the excess iron atoms in excess of  $x = 1.0$  substitute for the vanadium atoms on the  $M_2$  sites up to  $x = 2.0$  ( $Fe_2VS_4$ ) (13). Thus, the distance between the nearest-neighbor metal atoms is measured as  $\sim \frac{1}{4}c$  (Å), in which one metal atom at the  $M_1$  site is changed from vanadium to iron atom for  $x > 1.0$ . This metal-metal

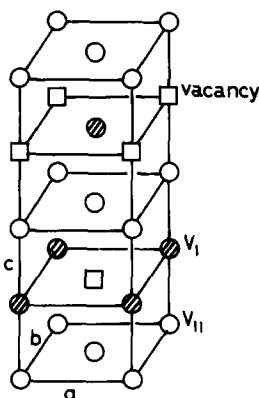


Fig. 1. Schematic arrangement of metal atoms in  $V_3S_4$  structure, where the intervening sulfur layers are omitted.  $V_1$  corresponds to  $M_1$  sites in the metal-deficient layers and  $V_{11}$  to  $M_2$  sites in the metal-full layers.

distance along the  $c$  axis is so short in the NiAs-like structures that strong metal-metal interactions can be expected. It is interesting to see how the Fe-V and the Fe-Fe interactions along the  $c$  axis affect the  $d$  state of iron and the magnetic properties.

In this paper, the magnetic susceptibility of  $Fe_xV_{3-x}S_4$  is studied in the composition range between  $x = 0$  and  $x = 2.0$ . The composition dependence of magnetic parameters, such as the effective magnetic moment, the Néel temperature, and the temperature-independent susceptibility, are determined from the measurement of high temperature susceptibility. Antiferromagnetic and weak ferromagnetic ordering at low temperatures are also reported. No magnetic studies of  $Fe_xV_{3-x}S_4$  have been performed in the composition range  $x > 1.0$ .

## Experimental

The samples of vanadium-iron sulfides were the same as in previous studies using Mössbauer spectroscopy (13) and Raman scattering (15). The sample preparation and chemical analysis were described in the previous reports (13, 15). The compositions of the specimens used in this experiment are  $V_3S_4$ ,  $Fe_{0.51}V_{2.49}S_4$ ,  $FeV_2S_4$ ,  $Fe_{1.5}V_{1.5}S_4$ ,  $Fe_{1.8}V_{1.2}S_4$ , and  $Fe_2VS_4$ . In spite of the changing rates of V and Fe, almost complete atomic orderings in  $FeV_2S_4$  and  $Fe_2VS_4$  could be confirmed by X-ray diffractometry with  $CrK\alpha$  radiation (16). The magnetic susceptibility was measured in the temperature range between 4.2 K and about 1300 K using a Cahn 1000 Electrobalance (Cahn Instrument, USA). Susceptibility data at high temperatures were fitted to the equation  $\chi = \chi_0 + C/(T + \theta_p)$ , where the first term represents the temperature-independent susceptibility and the second, a Curie-Weiss term. The magnitudes of  $\chi_0$  were determined by extrapolating the susceptibility to  $1/T = 0$ .

## Experimental Results

### 1. Magnetic Susceptibility at High Temperatures

The magnetic susceptibility between  $x = 0$  and  $x = 1.0$  is shown in Fig. 2, together with the reciprocal susceptibility. The susceptibility of  $\text{V}_3\text{S}_4$  shows a weak temperature dependence with a broad maximum at about 400 K and indicates that the compound has a very small localized magnetic moment. As seen in the figure,  $\text{FeV}_2\text{S}_4$  is antiferromagnetic with a Néel temperature of 140 K, which agrees well with a previous study (6). The susceptibility of  $\text{FeV}_2\text{S}_4$  obeys the Curie-Weiss law over the wide temperature range between 200 and 1200 K. No difference was detected between the susceptibility on heating and that on cooling below about 1200 K. However, it deviates from this law above approximately 1200 K and exhibits a hysteresis with respect to temperature, as seen in the insert of Fig. 2. This anomaly corresponds to a structural change from the  $\text{V}_3\text{S}_4$ -type to the metal-excess  $\text{CdI}_2$ -type structures; the temperature at which the anomaly occurs is in good agreement with the phase transition temperature observed in a high temperature X-ray study (10). The effective magnetic

moment of  $\text{FeV}_2\text{S}_4$  is  $3.2 \mu_B/\text{Fe}$ , assuming that only iron atoms exhibit a localized magnetic moment.  $\text{Fe}_{0.51}\text{V}_{2.49}\text{S}_4$  has two paramagnetic regions above and below about 700 K. The effective magnetic moment is  $2.49 \mu_B/\text{Fe}$  in the high temperature region above roughly 700 K and is of the same magnitude as that of  $\text{FeV}_2\text{S}_4$  below roughly 700 K. For  $\text{Fe}_{0.51}\text{V}_{2.49}\text{S}_4$ ,  $\chi_0$  is taken as  $\chi_0(T) = 0.49 \chi_A(T) + 0.51 \chi_B$ , where  $\chi_A$  is the susceptibility of  $\text{V}_3\text{S}_4$  and  $\chi_B$  is the temperature-independent susceptibility of  $\text{FeV}_2\text{S}_4$ . The Pauli paramagnetism in  $\text{V}_3\text{S}_4$  depends weakly on temperature and hence affects the  $\chi_0$  value of  $\text{Fe}_{0.51}\text{V}_{2.49}\text{S}_4$ .

The magnetic susceptibility in the composition range  $x > 1.0$  is shown in Fig. 3, together with the reciprocal susceptibility. The susceptibility of  $\text{Fe}_{1.8}\text{V}_{1.2}\text{S}_4$  is intermediate between that of  $\text{Fe}_{1.5}\text{V}_{1.5}\text{S}_4$  and  $\text{Fe}_2\text{VS}_4$ , and is omitted from the figure for clarity. The anomaly of the structure change is also clearly observed in the reciprocal susceptibility at high temperature. The insert of Fig. 3 shows the hysteresis in susceptibility associated with the phase transition of  $\text{Fe}_2\text{VS}_4$  from the  $\text{V}_3\text{S}_4$ -type to the  $\text{CdI}_2$ -type structures. The phase transition temperature decreases with increasing iron content, as is shown in Fig. 4 in con-

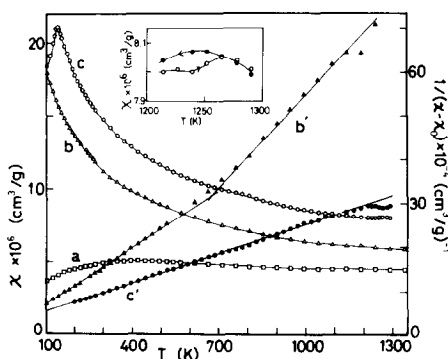


FIG. 2. Magnetic susceptibility of  $\text{Fe}_x\text{V}_{3-x}\text{S}_4$ : (a)  $\text{V}_3\text{S}_4$ , (b)  $\text{Fe}_{0.51}\text{V}_{2.49}\text{S}_4$ , and (c)  $\text{FeV}_2\text{S}_4$ .  $b'$  and  $c'$  represent the reciprocal susceptibility of  $\text{Fe}_{0.51}\text{V}_{2.49}\text{S}_4$  and  $\text{FeV}_2\text{S}_4$ , respectively. The insert shows the hysteresis of the susceptibility in  $\text{FeV}_2\text{S}_4$ .

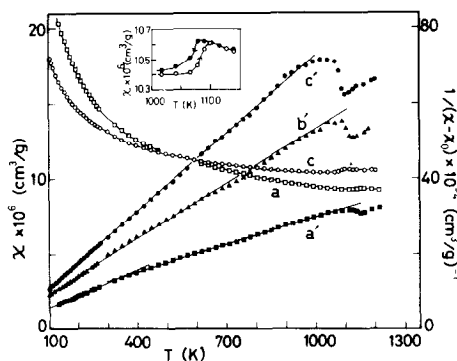


FIG. 3. Magnetic susceptibility of  $\text{Fe}_x\text{V}_{3-x}\text{S}_4$ : (a)  $\text{Fe}_{1.5}\text{V}_{1.5}\text{S}_4$  and (c)  $\text{Fe}_2\text{VS}_4$ .  $a'$ ,  $b'$ , and  $c'$  represent the reciprocal susceptibility of  $\text{Fe}_{1.5}\text{V}_{1.5}\text{S}_4$ ,  $\text{Fe}_{1.8}\text{V}_{1.2}\text{S}_4$ , and  $\text{Fe}_2\text{VS}_4$ , respectively. The insert shows the hysteresis of the susceptibility in  $\text{Fe}_2\text{VS}_4$ .

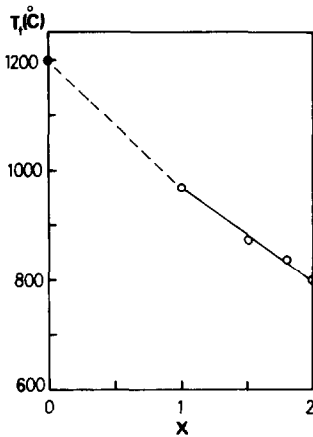


FIG. 4. Phase transition temperature determined from the middle point of the hysteresis. The solid circle refers to the transition temperature of  $V_3S_4$  determined from DTA (17).

junction with that of  $V_3S_4$ , as determined by a DTA study (17). The susceptibility in this composition range also obeys the Curie-Weiss law over a wide temperature range. The temperature dependence, however, weakens with increasing  $x$  and therefore, the magnitude of the effective magnetic moment decreases with increasing iron content. The susceptibility of  $Fe_{1.5}V_{1.5}S_4$  covers two paramagnetic regions which have slightly different effective magnetic moment:  $2.61 \mu_B$  per  $M_1$ -site iron atom below 340 K and  $3.08 \mu_B$  per  $M_1$ -site iron atom above 340 K, although the susceptibility for both  $Fe_{1.8}V_{1.2}S_4$  and  $Fe_2VS_4$  can be represented by only one magnetic moment over the whole temperature range. The composition dependence of the magnetic parameters of  $Fe_xV_{3-x}S_4$ , e.g., the effective magnetic moment, the temperature independent susceptibility, the asymptotic Curie temperature and the Néel temperature, are shown in Fig. 5. In the figure, two regions are roughly outlined, which join at the composition  $x = 1.0$ , as indicated by the different dependences of the magnetic parameters on composition. In the composition range  $x < 1.0$  the Néel temperature

increases with increasing  $x$ , in agreement with a previous observation (3); this is associated with the increasing number of the magnetic iron atoms at the  $M_1$  sites. The effective magnetic moment of the iron atom, which was calculated by assuming that vanadium atoms have no localized magnetic moment, appears to remain unchanged in magnitude in that range, being the same as the temperature-independent susceptibility. In the composition range  $x > 1.0$  both the Néel temperature and the effective magnetic moment decrease with in-

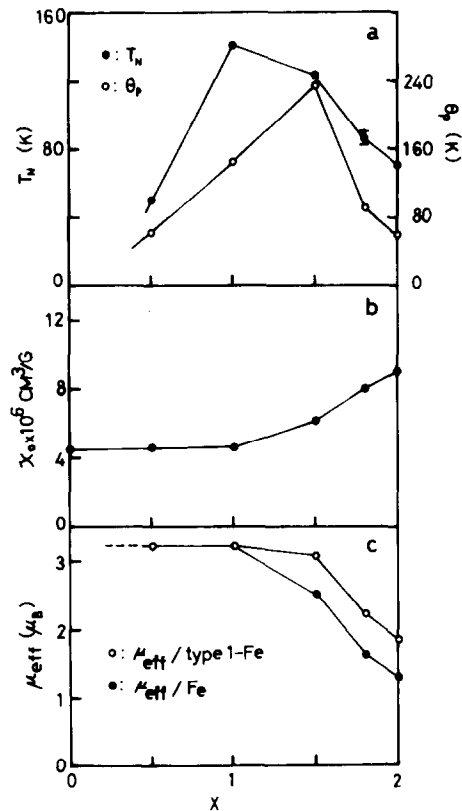


FIG. 5. Composition dependence of magnetic parameters in  $Fe_xV_{3-x}S_4$ . In (a) the Néel temperature (solid circles) and asymptotic Curie temperatures (open circles) are shown. Temperature-independent susceptibility and effective magnetic moments are shown in (b) and (c), respectively. In (c) solid circles represent the average effective magnetic moment per an iron; open circles, the effective magnetic moment per a  $M_1$ -site iron atom.

creasing iron content, particularly near the composition  $x = 2.0$ . The average effective magnetic moment of an iron atom is  $1.3 \mu_B$  in  $\text{Fe}_2\text{VS}_4$ . Even if one can assume that only the iron atoms at the  $M_1$  sites have a localized magnetic moment, the effective magnetic moment is  $1.8 \mu_B$  per  $M_1$ -site iron atom, significantly below that expected from a ferrous iron in a high-spin state. The temperature-independent susceptibility increases gradually with increasing  $x$  in the composition range  $x > 1.0$ .

The composition dependence of the lattice parameters is shown in Fig. 6; note that the  $c$  parameter also considerably decreases at near  $x = 2.0$ .

## 2. Magnetic Ordering at Low Temperatures

As is shown in Fig. 7 the compound  $\text{Fe}_{0.51}\text{V}_{2.49}\text{S}_4$  with composition intermediate between  $\text{V}_3\text{S}_4$  and  $\text{FeV}_2\text{S}_4$  exhibits weak ferromagnetism at temperatures below about 40 K, when the specimen is cooled to 4.2 K under an applied field of 10.6 kOe. The thermomagnetic curves in the figure show, however, that the material is basically antiferromagnetic with the Néel temperature of 50 K which is slightly higher than a previously quoted result (3). After cooling in the field, the weak spontaneous magnetization,  $0.02 \text{ G} \cdot \text{cm}^3/\text{g}$ , has been found from the field dependence of the magnetization at 4.2 K, as shown in the insert of Fig. 7. However, no spontaneous magnetization is observed for  $\text{V}_3\text{S}_4$  and  $\text{FeV}_2\text{S}_4$ , nor for  $\text{Fe}_{0.51}\text{V}_{2.49}\text{S}_4$  after cooling the specimen in the zero field.

Weak ferromagnetism also exists in the compounds of composition  $x > 1.0$ .  $\text{Fe}_{1.5}\text{V}_{1.5}\text{S}_4$  is antiferromagnetic with the Néel temperature of 123 K and shows weak ferromagnetism below 11 K after cooling the specimen in the magnetic field, as seen from the thermomagnetic curve of Fig. 8 (small solid circles) and also as seen from the temperature dependence of the square

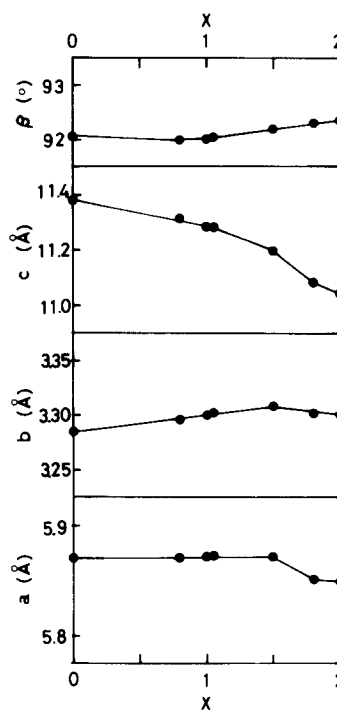


FIG. 6. Composition dependence of the lattice parameters in  $\text{Fe}_x\text{V}_{3-x}\text{S}_4$ . The length of the  $c$  axis particularly decreases with increasing  $x$ .

of the spontaneous magnetization in the insert of Fig. 8. The magnetization (susceptibility) represented by open circles in the figure is a part of the magnetization which varies linearly on field strength, that is, the quantity calculated after subtracting the spontaneous magnetization from the magnetization. It exhibits a broad maximum close to 16 K.  $\text{Fe}_{1.8}\text{V}_{1.2}\text{S}_4$  also exhibits weak ferromagnetism after cooling the specimen in the field (Fig. 9). The spontaneous magnetization, however, appears to occur with a very weak long tail, even at about 85 K, as seen in the insert of Fig. 9. Near this temperature, the susceptibility has a broad cusp probably masked by the ferromagnetic tail. This suggests that  $\text{Fe}_{1.8}\text{V}_{1.2}\text{S}_4$  is also basically antiferromagnetic. The part of the magnetization that depends linearly on field strength has a broad maximum about 35 K, similar to that in  $\text{Fe}_{1.5}\text{V}_{1.5}\text{S}_4$ .

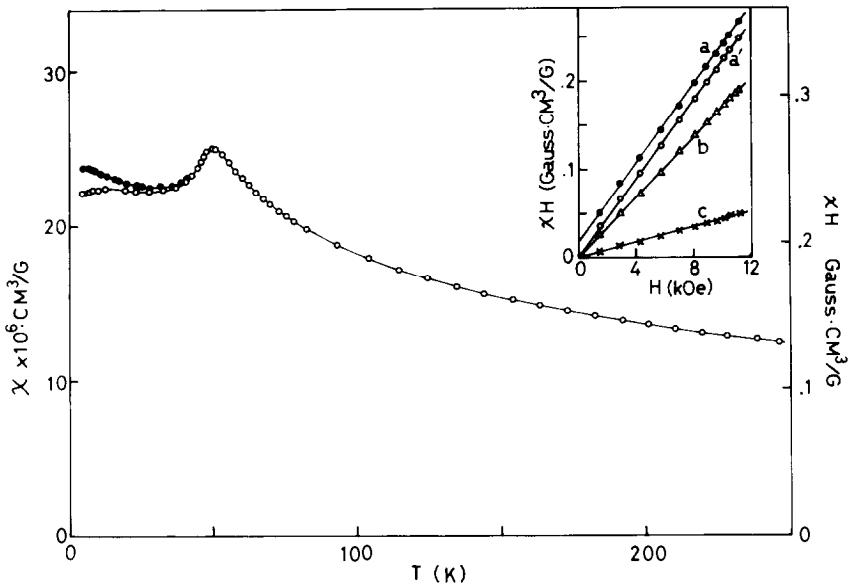


FIG. 7. Magnetic susceptibility (magnetization) of  $\text{Fe}_{0.51}\text{V}_{2.49}\text{S}_4$  at low temperatures. A thermomagnetic curve on cooling under a field of 10.6 kOe is represented by solid circles and another curve represented by open circles corresponds to a thermomagnetic curve after cooling the specimens in zero field. The insert shows the field-strength dependence of the magnetization at 4.2 K. The magnetization after cooling in the field and in the zero field are indicated by a and a', respectively, together with that of  $\text{V}_3\text{S}_4$  (c) and  $\text{FeV}_2\text{S}_4$  (b).

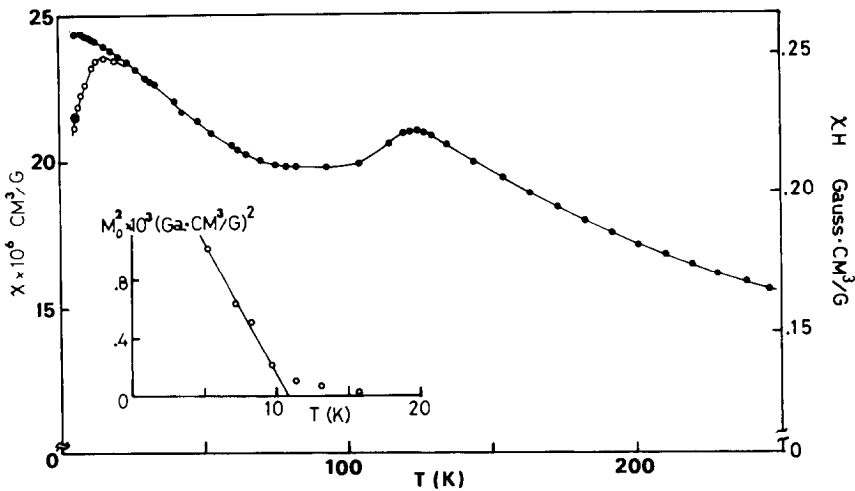


FIG. 8. Magnetic susceptibility (magnetization) of  $\text{Fe}_{1.5}\text{V}_{1.5}\text{S}_4$ . Solid circles correspond to the susceptibility after cooling in a field of 10.6 kOe and a large solid circle to that after cooling in the absence of a field at 4.2 K. Open circles refer to magnetization (susceptibility) after subtracting the spontaneous magnetization. Temperature dependence of square of spontaneous magnetization is shown in the insert.

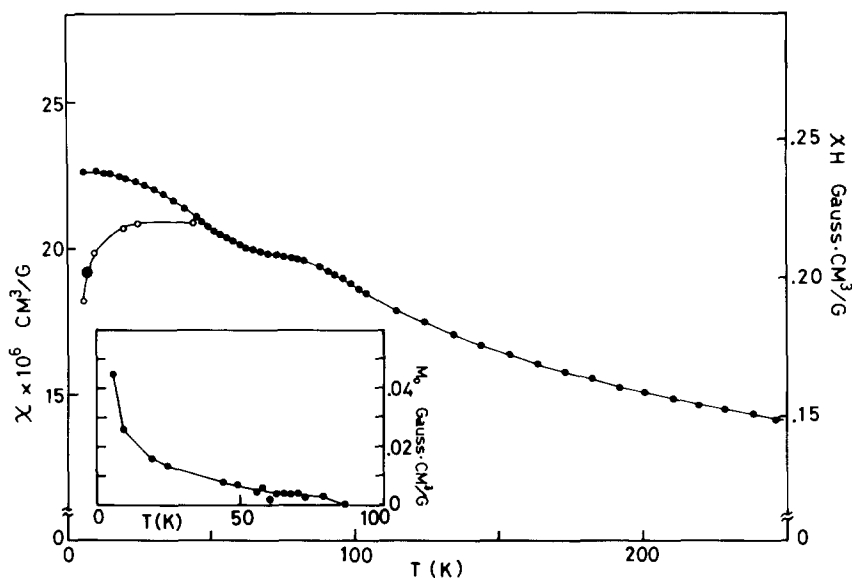


FIG. 9. Magnetic susceptibility (magnetization) of  $\text{Fe}_{1.8}\text{V}_{1.2}\text{S}_4$ . Small solid circles correspond to the susceptibility after cooling in a field of 10.6 kOe and a large solid circle to that after cooling in zero field at 4.2 K. Open circles refer to magnetization (susceptibility) after subtracting the spontaneous magnetization. The temperature dependence of the spontaneous magnetization is shown in the insert.

The thermomagnetic curves of  $\text{Fe}_2\text{VS}_4$ , as shown in Fig. 10, appear to be weakly ferromagnetic. The field cooling effect is also observed, as indicated by solid and open circles in the figure. However, the field-strength dependence of the magnetization at 4.2 K, as shown in Fig. 11, indicates that the compound has a spontaneous magnetization even after cooling the specimen in zero field as well as in a field of 10.6 kOe, and that the magnitudes for the both cases are larger by one order magnitude than those of the other  $\text{Fe}_x\text{V}_{3-x}\text{S}_4$  compounds. The temperature dependence of the spontaneous magnetization after cooling the specimen in the field is shown in Fig. 12. The Curie temperature,  $T_c = 70$  K, which is rather higher than the others, is determined by the manner shown in the insert of Fig. 12. The part of the magnetization depending linearly on field strength, as seen in the insert of Fig. 10, indicates that there exists a sharp cusp in the susceptibility at 70 K which agrees with  $T_c$ . It suggests that

$\text{Fe}_2\text{VS}_4$  is basically an antiferromagnet accompanied by a weak ferromagnetism.

## Discussion

### 1. Reduced Magnetic Moment of Fe

In the system,  $\text{VS}-\text{VS}_2$ , the  $d$  electrons of vanadium atoms in the metal-full layers are completely delocalized. However, vanadium atoms in the metal-deficient layers have a large localized magnetic moment in  $\text{V}_5\text{S}_8$  and  $\text{V}_{1+x}\text{S}_2$  ( $0.08 \leq x \leq 0.19$ ) phases (18–22). Since the  $d$  electrons of iron in sulfides have a greater tendency to localize than do those of vanadium, it seems natural to assume that in  $\text{FeV}_2\text{S}_4$ , only those iron atoms that occupy the metal sites in the metal-deficient layers, have a magnetic moment. From this assumption, it is deduced that the effective magnetic moment of iron in  $\text{FeV}_2\text{S}_4$  is  $3.2 \mu_B$ . The result differs from previous data (6, 7). According to Muranaka and Takada (6) the magnetic sus-

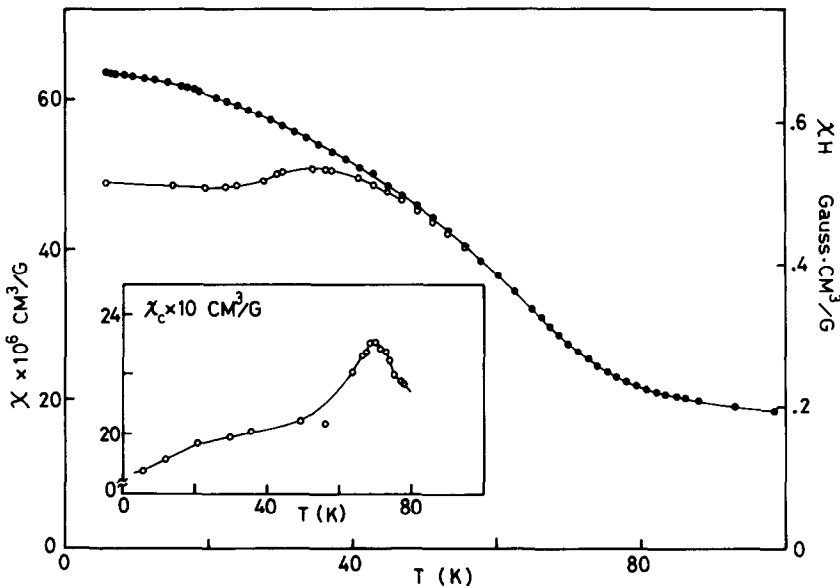


FIG. 10. Magnetic susceptibility (magnetization) of  $\text{Fe}_2\text{VS}_4$ . Solid circles correspond to the susceptibility after cooling in a field of 10.6 kOe and open circles to that after cooling in zero field. The insert shows susceptibility after subtracting the spontaneous magnetization.

ceptibility is characterized by three paramagnetic regions with different effective magnetic moments in each temperature range:  $3.40 \mu_B$  between 140 and 300 K,  $4.23 \mu_B$  between 300 and 850 K, and  $5.32 \mu_B$  between 850 and 1240 K. The effective magnetic moment of the present study almost agrees with the previous data in the lower temperature range and also with

results obtained on a single crystal (6), but disagrees with the high temperature result. This difference in the present and previous results may be due to the difference in the magnitudes of  $\chi_0$ : the previous  $\chi_0$ , 2.8 emu/g, is smaller than the present  $\chi_0$ , 4.0 emu/g. It should be noted that the phase transition from the  $\text{V}_3\text{S}_4$ -type to the metal-excess  $\text{CdI}_2$ -type structures does not occur at 820 K (6) but in the temperature range between about 1200 and 1270 K, as seen in the insert of Fig. 2.

As mentioned previously, iron atoms substitute for vanadium atoms of the  $M_2$  sites rather than in the  $M_1$  sites for the composition range  $x > 1.0$ . This is reflected in the composition dependence of the magnetic properties and the lattice parameters. The composition dependence of the effective magnetic moment strongly suggests that the changeover of the nearest metal atoms along the  $c$  axis from V to Fe significantly affects the  $d$  state of the  $M_1$ -site iron. Next, we will discuss the  $d$  state of iron atoms on the basis of the magnetic and

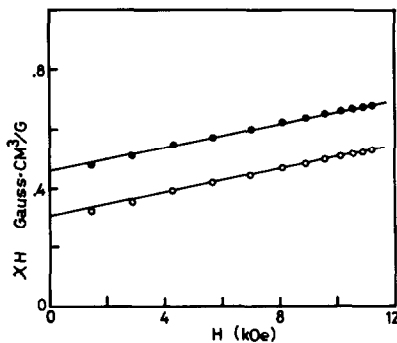


FIG. 11. Field-strength dependence of magnetization in  $\text{Fe}_2\text{VS}_4$  at 4.2 K. Solid and open circles represent the magnetizations after cooling in a field of 10.6 kOe and in zero field, respectively.



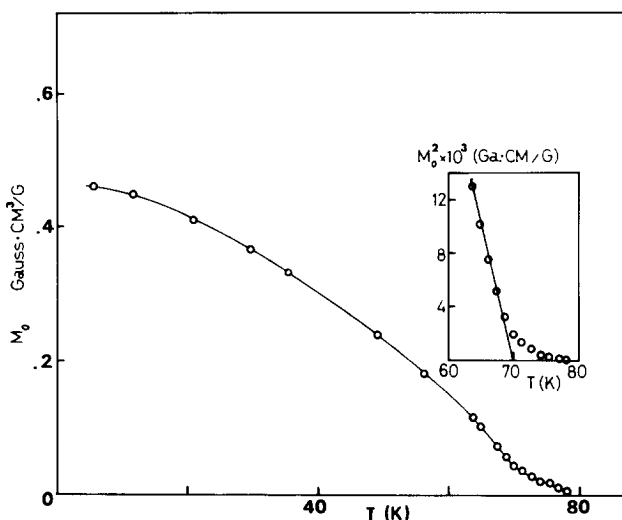


FIG. 12. Temperature dependence of the spontaneous magnetization in  $\text{Fe}_2\text{VS}_4$ . The insert shows the temperature dependence of the square of the spontaneous magnetization near the Curie temperature.

structural data in addition to previous data of Mössbauer effect.

The magnitude of effective magnetic moment in  $\text{Fe}_x\text{V}_{3-x}\text{S}_4$  is far below that expected for  $\text{Fe}^{2+}$  in a high-spin state. This suggests an extended wave function for  $d$  electrons of the iron atom. Strong direct metal-metal interaction or indirect metal-anion-metal interaction can cause  $d$  electrons to be itinerant, as discussed by Goodenough (23, 24) and recently Fatseas and Goodenough (25). In  $\text{V}_3\text{S}_4$ , the vanadium atoms in the metal-filled layers are associated with itinerant  $d$  electrons, probably due to large overlaps of  $3d$  wave functions extended in the metal layers. The V-V distance between the metal layers is so short, 2.91 Å, that the strong V-V interactions along the  $c$  axis are expected to be largely responsible for the nonmagnetic character of the vanadium atoms in the metal-deficient layers as observed in the magnetic susceptibility. In the compound,  $\text{Fe}_x\text{V}_{3-x}\text{S}_4$ , it is likely that the Fe-V or Fe-Fe distance along the  $c$  axis is probably not much larger than the V-V distance in  $\text{V}_3\text{S}_4$ , because the  $c$  parameter decreases gradu-

ally with increasing iron content and rapidly decreases near the composition  $x = 2.0$ , although the small monoclinic distortion does not allow one to estimate the precise metal-metal distance solely from the  $c$  parameter. Thus, the Fe-Fe distance along the  $c$  axis, in the composition range  $x > 1.0$ , seems to be rather smaller than the critical separation of about 3 Å (24), within which minority-spin  $d$  electrons of  $\text{Fe}^{2+}$  (a  $d$  electron with a spin opposite to five-parallel spins in half-filled  $d$  orbitals) are expected to be collective at least for the Fe-Fe pairs along the  $c$  axis.

The Fe-S distance in  $\text{Fe}_x\text{V}_{3-x}\text{S}_4$  is inferred from the composition dependence of the lattice parameters (Fig. 6). The V-S distances in the compound  $\text{VS}_{1.47}$ , which also has the  $\text{V}_3\text{S}_4$  structure, are between 2.397 Å at the  $M_2$  site and 2.406 Å at the  $M_1$  site which are averaged values at the respective site (12). The V-S distance in stoichiometric  $\text{V}_3\text{S}_4$ , averaging approximately 2.41 Å, which was deduced by interpolation from structure data in  $\text{VS-VS}_2$  (12, 26, 27), is much smaller than the Fe-S distance in  $\text{Fe}_7\text{S}_8$ , 2.449 Å (28). Thus, the Fe-S dis-

tance in  $\text{Fe}_x\text{V}_{3-x}\text{S}_4$  may be much smaller than that in  $\text{Fe}_7\text{S}_8$ . For such a Fe-S distance, relatively strong  $\sigma$  bonding between Fe and S may be present in the vanadium-containing iron sulfides; therefore, Fe-S-M interactions ( $M = \text{V}$  or Fe) may make  $d$  electrons with  $e_g$  symmetry collective, so as to introduce a narrow  $\sigma^*$  bands (25).

A previous study of the Mössbauer effect in  $\text{Fe}_x\text{V}_{3-x}\text{S}_4$  indicates that the isomer shift of the iron atoms at the  $M_1$  sites decreases smoothly with increasing iron content from  $0.735 \pm 0.005$  to  $0.630 \pm 0.005$  mm/sec and, therefore, no abrupt change of the  $d$  state is expected over the whole composition range (13). The values are rather smaller than those of high-spin ferrous irons in ionic crystals and may be associated with itinerant  $\sigma^*$  electrons in a high-spin configuration (25). On the other hand, the iron atom at the  $M_2$  site which is neighbor to six metal atoms in the metal-full layer, as well as to one iron atom in the adjacent metal-deficient layer along the  $c$  axis, has a lower value of the isomer shift by about 0.1 mm/sec than that of the iron atom at the  $M_1$  site. The iron atom at the  $M_2$  site may, therefore, have a more extended  $d$  wave function and may have a much more reduced magnetic moment than that of the iron atom at the  $M_1$  site. However, it is not impossible that the iron at the  $M_2$  site is in a low-spin state of  $\text{Fe}^{2+}$ , as suggested in a study of  $\text{Fe}_{0.1}\text{V}_{0.9}\text{S}_2$  (4, 5).

Thus, an explanation is proposed for the intermediate magnitude of the magnetic moment of the iron atom at the  $M_1$  site. The direct and the indirect interactions may make the  $d$  electrons collective in part and they also reduce the intraatomic interaction on the iron atom significantly, resulting in an intermediate magnitude of magnetic moment on the iron atom. On increasing the iron content beyond  $x = 1.0$ , the direct interactions between metal layers become stronger and result in a gradual decrease of the magnitude of the magnetic moment. As

seen in the gradual increase of  $\chi_0$  (Fig. 5), they may also affect the  $d$ -band structure significantly. The composition dependence of the effective magnetic moment and the  $c$  parameter suggest that strong Fe-Fe bonding exists along the  $c$  axis in  $\text{Fe}_x\text{V}_{3-x}\text{S}_4$ , as suggested by a Raman scattering experiment (15).

## 2. Antiferro- and Weak Ferromagnetism

All the compounds of  $\text{Fe}_x\text{V}_{3-x}\text{S}_4$  seem to be basically antiferromagnetic. However, they show weak ferromagnetism at low temperatures, excepting  $\text{V}_3\text{S}_4$  and  $\text{FeV}_2\text{S}_4$ . The weak ferromagnetism of  $\text{Fe}_{0.51}\text{V}_{2.49}\text{S}_4$  is rather curious because the compound is intermediate in composition between antiferromagnetic  $\text{V}_3\text{S}_4$  and  $\text{FeV}_2\text{S}_4$ . Since V and Fe atoms are thought to be distributed randomly at the  $M_1$  sites within the metal-deficient layers, the field cooling effect for  $\text{Fe}_{0.51}\text{V}_{2.49}\text{S}_4$  suggests that the ferromagnetism is due to short-range ordering and, therefore, ferromagnetic clusters of iron atoms are formed in the antiferromagnetic matrix when the specimen is cooled under the field. Similar phenomena are observed in metal alloys such as Cu-Mn (29). Ferromagnetic clusters may exist as long as ferromagnetic interactions are present between the iron atoms at any  $M_1$  sites. Ferromagnetic interactions probably occur in  $\text{Fe}_{0.51}\text{V}_{2.49}\text{S}_4$ , because the magnetic structure of  $\text{V}_5\text{S}_8$  (21), as studied by a neutron diffraction experiment, suggests that there exist ferromagnetic interactions between the vanadium atoms in the metal-deficient layers of the structure, in addition to antiferromagnetic ones. The structure of  $\text{V}_5\text{S}_8$  is very similar to that of  $\text{V}_3\text{S}_4$  except for vacancy ordering within alternative metal-deficient layers.  $\text{FeV}_2\text{S}_4$  can never be ferromagnetic because the  $M_1$  sites are fully occupied by iron atoms, all of which have stronger basic antiferromagnetic interactions than ferromagnetic ones.

The weak ferromagnetism of  $\text{Fe}_{1.5}\text{V}_{1.5}\text{S}_4$

and  $\text{Fe}_{1.8}\text{V}_{1.2}\text{S}_4$  can be considered to be similar to that in  $\text{Fe}_{0.51}\text{V}_{2.49}\text{S}_4$ . However, the ferromagnetism for the both compounds may not be associated with the iron atoms at the  $M_1$  sites but with those at the  $M_2$  sites, because in the metal-full layers, the iron and vanadium atoms may be distributed randomly, whereas in the metal-deficient layers, the  $M_1$  sites are fully occupied by iron atoms which may contribute to anti-ferromagnetic ordering.

In  $\text{Fe}_2\text{VS}_4$ , the weak ferromagnetism differs in several points from that in the other compounds in  $\text{Fe}_x\text{V}_{3-x}\text{S}_4$ . These differences are (1) the compound has a relatively high Curie temperature which agrees with the Néel temperature; (2) the magnetization is larger by one order of magnitude than that in the other compounds; (3) the spontaneous magnetization occurs even after cooling the specimen in the zero field. Thus,  $\text{Fe}_2\text{VS}_4$  exhibits long-range ferromagnetic ordering, which is different from a short-range ordering of the ferromagnetic clusters. It was reported that a compound of  $\text{Fe}_2\text{TiS}_4$  which has an isomorphous structure of  $\text{V}_3\text{S}_4$  was ferrimagnetic below 285 K (30). However, for  $\text{Fe}_2\text{VS}_4$  this is not the case, because in  $\text{Fe}_2\text{VS}_4$  the iron atoms at the  $M_2$  sites may have considerably reduced magnetic moments in comparison with those of iron atoms at the  $M_1$  sites and, therefore, a ferrimagnetic spin arrangement between the iron atoms at both sites will produce a significantly larger magnetization than that observed in the present experiment. Therefore, it seems that two possible explanations exist concerning the origin of the weak ferromagnetism. One is that the ferromagnetism is due to a canted-spin anti-ferromagnetism and the other is that the ferromagnetism is ascribed to a ferromagnetic ordering of small magnetic moments at the  $M_2$  sites which may be coupled magnetically to the magnetic moments of  $M_1$ -site iron atoms below the Néel temperature. Unfortunately, the origin of the weak

ferromagnetism of  $\text{Fe}_2\text{VS}_4$  cannot be clarified in this stage. A more detailed study using single crystals is necessary.

### Acknowledgments

The authors thank Dr. M. Umehara and Dr. H. Nakazawa for their helpful discussions. Thanks are also due to the late Prof. M. Nakahira and to Dr. I. Kawada for their encouragement in the present study.

### References

1. Y. KITAOKA AND H. YASUOKA, *J. Phys. Soc. Japan* **48**, 1460 (1980).
2. E. HIRAHARA AND M. MURAKAMI, *J. Phys. Chem. Solids* **7**, 281 (1958).
3. Y. OKA, K. KOSUGE, AND S. KACHI, *Mat. Res. Bull.* **15**, 521 (1980).
4. F. J. DISALVO, M. EIBSCHÜTZ, C. CROS, D. W. MURPHY, AND J. W. WASZCZAK, *Phys. Rev. B* **19**, 3441 (1979).
5. M. EIBSCHÜTZ, D. W. MURPHY, AND F. J. DISALVO, *Phys. Status Solidi B* **99**, 145 (1980).
6. S. MURANAKA AND T. TAKADA, *J. Solid State Chem.* **14**, 291 (1975).
7. B. C. MORRIS, V. JOHNSON, R. H. PLOVNIC, AND A. WOLD, *J. Appl. Phys.* **40**, 1299 (1969).
8. H. WADA, *Bull. Chem. Soc. Japan* **52**, 2130 (1979).
9. H. WADA, *Bull. Chem. Soc. Japan* **51**, 1368 (1978).
10. H. WADA, *Bull. Chem. Soc. Japan* **52**, 2918 (1979).
11. H. WADA, *Bull. Chem. Soc. Japan* **53**, 668 (1980).
12. I. KAWADA, M. NAKANO-ONODA, M. ISHII, M. SAEKI, AND M. NAKAHIRA, *J. Solid State Chem.* **15**, 246 (1975).
13. H. NOZAKI, H. WADA, AND H. YAMAMURA, *Solid State Commun.* **44**, 63 (1982).
14. I. KAWADA AND H. WADA, *Phys. Status Solidi B* **105**, 223 (1981).
15. M. ISHII, H. WADA, H. NOZAKI, AND I. KAWADA, *Solid State Commun.* **42**, 605 (1982).
16. N. NAKAZAWA, private communication.
17. Y. OKA, K. KOSUGE, AND S. KACHI, *J. Solid State Chem.* **23**, 11 (1978).
18. A. B. DE VRIES AND C. HAAS, *J. Phys. Chem. Solids* **34**, 651 (1973).
19. B. G. SILBERNAGEL, R. B. LEVY, AND F. R. GAMBLE, *Phys. Rev. B* **11**, 4563 (1975).
20. H. NOZAKI, M. UMEHARA, Y. ISHIZAWA, M. SAEKI, T. MIZOGUCHI, AND M. NAKAHIRA, *J. Phys. Chem. Solids* **39**, 851 (1978).

21. S. FUNAHASHI, H. NOZAKI, AND I. KAWADA, *J. Phys. Chem. Solids* **42**, 1009 (1981).
22. H. KATSUTA, R. B. MCLELLAN, AND K. SUZUKI, *J. Phys. Chem. Solids* **40**, 1089 (1979).
23. J. B. GOODENOUGH, *Mat. Res. Bull.* **6**, 967 (1971).
24. J. B. GOODENOUGH, *Mat. Res. Bull.* **13**, 1305 (1978).
25. A. FATSEAS AND J. B. GOODENOUGH, *J. Solid State Chem.* **33**, 219 (1980).
26. M. NAKANO-ONODA, S. YAMAOKA, Y. YUKINO, K. KATO, AND I. KAWADA, *J. Less-Common Metals* **44**, 341 (1976).
27. M. NAKANO-ONODA AND M. NAKAHIRA, *J. Solid State Chem.* **30**, 283 (1979).
28. M. TOKONAMI, K. NISHIGUCHI, AND N. MORIMOTO, *Amer. Miner.* **57**, 1066 (1972).
29. P. A. BECK, *J. Less-Common Metals* **28**, 193 (1972).
30. S. MURANAKA, *J. Phys. Soc. Japan* **35**, 1553 (1973).